Evolution of stress in evaporated silicon dioxide thin films

Ming Fang (方 明)[1,2*], Dafei Hu (胡达飞)[1,2], and Jianda Shao (邵建达)[1]

[1] *Key Laboratory of Material Science and Technology for High Power Lasers, Shanghai Institute of Optics and Fine Mechanics, Chinese Academy of Sciences, Shanghai 201800, China*

[2] *Graduate School of Chinese Academy of Sciences, Beijing 100049, China*

[*] *E-mail: fm@siom.ac.cn*

Received March 31, 2009

The evolution of stress in evaporated SiO_2, used as optical coatings, is investigated experimentally through *in situ* stress measurement. A typical evolution pattern consisting of five subprocedures (thin film deposition, stopping deposition, cooling, venting the vacuum chamber, and exposing coated optics to the atmosphere) is put forward. Further investigations into the subprocedures reveal their features. During the deposition stage, the stresses are usually compressive and reach a stable state when the deposited film is thicker than 100 nm. An increment of compressive stress value is observed with the decrease of residual gas pressure or deposition rate. A very low stress of –20 MPa is formed in SiO_2 films deposited at 3×10^{-2} Pa. After deposition, the stress increases slightly in the compressive direction and is subject to the stabilization in subsequent tens of minutes. In the process of venting and exposure, the compressive component increases rapidly with the admission of room air and then reaches saturation, followed by a logarithmic decrement of the compressive state in the succeeding hours. An initial discussion of these behaviors is given.

OCIS codes: 310.3840, 160.4670.

doi: 10.3788/COL20100801.0119.

It is well known that excessive residual stress can cause crack, deformation, or even peeling off in thin films, thereby greatly limiting the properties and the reliability of thin-film-based devices[1]. For precision optics, the stress could bend the coated optics, which would change the energy distribution of the light beam for low-frequency modulation[2]. In view of this, much work has been concentrated on the originality of stress[3], thermal stress[4], relationship between film stress and structure[5,6], effects of the deposition process[7–10], annealing effects, and exposure to various environments on the stress in the films[11]. Although the results were based on *ex situ* stress measurement, they have promoted the production of precision optics. There have been developments in the study of high-precision optics. However, we need to enhance our knowledge on more accurate control of all the components of residual stress. Real-time stress monitoring and control are needed for the overall process.

In situ stress measurement has been widely used in applications such as electronics[12], micro electromechanical system, and research into the origin of stress[13]. A reversible compressive stress that develops during Volmer-Weber growth of polycrystalline Cu films has been observed[14,15]. Thurn *et al.* investigated the mechanical response of plasma-enhanced chemical vapor deposition SiO_2 to thermal cycling[16], which showed that a structure-dependent stress state during the thermal cycling was applied to the films. Comparatively, little attention has been devoted to the stress evolution in the preparation of optical coatings[17]. Ennos studied the stress evolution in the growth of ZnS, MgF_2, Al, and Cr, among others[18]. This was the first time that we were provided a direct observation of stress in optical coating growth. Such an examination is a necessary step in understanding and predicting the behavior of dielectric films during preparation at a level comparable to precision optics requirement.

To date, the deposition technology and the leading material used in optical coating have made great progress. For instance, SiO_2 films prepared by electron-beam evaporation have been widely used in optics as a low-index material with high laser-induced damage threshold. Its stress is one of the major concerns in these applications and has been studied by *ex situ* stress measurement[19]. It is concluded that the absorption of water molecules leads to an increase in the compressive stress component in the films when the films are brought into the ambient air[8,17,20]. A tensile component attributed to hydration-induced stress decreases linearly as the logarithm of the aging time increases.

In this letter, we continuously observe the evolution of stress in the SiO_2 film preparation to explore the subprocedure-level control of stress evolution. The purpose of this work is either to make SiO_2 films free of stresses or to give them a controlled stress level to balance the stresses in materials associated with SiO_2 in an optical multilayer structure.

SiO_2 monolayers were grown on borate glass sheets (D263T, Schott, $50\times10\times0.21$(mm)). The substrates were sequentially rinsed in acetone, ethanol, and distilled water. SiO_2 bulk material with a purity of 99.99% was used as target and evaporated by electron-beam. The sweep of the electron beam and the proportional-integral-derivative (PID)-controlled power supply were applied to ensure a stable deposition rate. The chamber was pumped to a base pressure of 3×10^{-3} Pa before deposition. High-purity oxygen (99.99%) was charged to control the oxygen partial pressure for oxidation and residual gas pressure. The ambient temperature was controlled by the PID power to a stable state and the measuring point was in the middle of the heater and sub-

strates. The film thickness was controlled by a quartz crystal-controlled oscillator (QCCO) (MDC360, Maxtek). The deposition angle of vapor was about 37°. The uniformity of film thickness in the glass sheet was better than ±1.5%.

To investigate the growth stress of SiO_2, a large-scale deposition condition was chosen. The deposition rate ranged from 0.3 to 0.7 nm/s. The residual gas pressure varied from base pressure to 3×10^{-2} Pa. The ambient temperature ranged from 50 to 200 °C. The film thickness was set to about 340 nm.

To investigate the overall process stress evolution, SiO_2 film (deposited under 3×10^{-3} Pa, 200 °C, and 0.5 nm/s) was uninterruptedly observed from the beginning of deposition up to the time it was taken off the holder. The sample was kept under the deposition condition (3×10^{-3} Pa, 200 °C) after deposition for 3000 s, and then the ambient temperature (3×10^{-3} Pa) was lowered from 200 to 68 °C in about 5000 s. A fast venting process was applied and then the sample was exposed to the atmospheric environment (27 °C, relative humidity 60%) for 4000 s.

To investigate the venting and exposure process in detail, slow venting and film quality monitoring by QCCO were applied to the SiO_2 deposited under the conditions of 2×10^{-2} Pa, 200 °C, and 0.5 nm/s. The lifespan of the quartz crystal was 94%. The beginning temperature for venting was 36 °C, close to the temperature of cooling water for the quartz crystal oscillator. The whole venting process had been taken more than three hours, which was far longer than those of the standard routines. The two subprocedures were started as the main valve was being closed. In the first 2000 s, the vacuum chamber was charged by self-leaking. Slow venting was then done via a small opening of the process chamber in the first phase of the ventilation process. Residual gas pressure rose from 2 to 1000 Pa in the next 580 s. After venting, the sample was exposed to the atmosphere (27 °C, relative humidity 60%) for 8.3 h. The measurement of *in situ* stress measurement based on wafer curvature measurement by optical deflection of two parallel light beams has been described previously[21].

Figure 1(a) shows the influence of the residual gas pressure on the growth stress of SiO_2. The dotted line in the upper figure is the tensile and compressive demarcation line. Under all conditions, the growth stress of SiO_2 showed a compressive state, while the lower pressure showed a higher stable compressive stress. For lower growth gas pressure, a compressive stress peak emerged when the thickness was small. This phenomenon was also reported in the *in situ* stress observation of HfO_2 films[21]. Leaving the area of stress changing dramatically, a growth stress was obtained with a thickness of larger than 100 nm. The thickness is quite important for research work on surface stress and structure-dependent stress.

The influences of deposition rate and ambient temperature on the growth stress of SiO_2 are shown in Figs. 1(b) and (c), respectively. Although SiO_2 shows a compressive growth stress in all conditions, it is easy to see that in these deposition conditions, SiO_2 is more greatly affected during the early stage of growth than during the stable stress state, especially in the case of

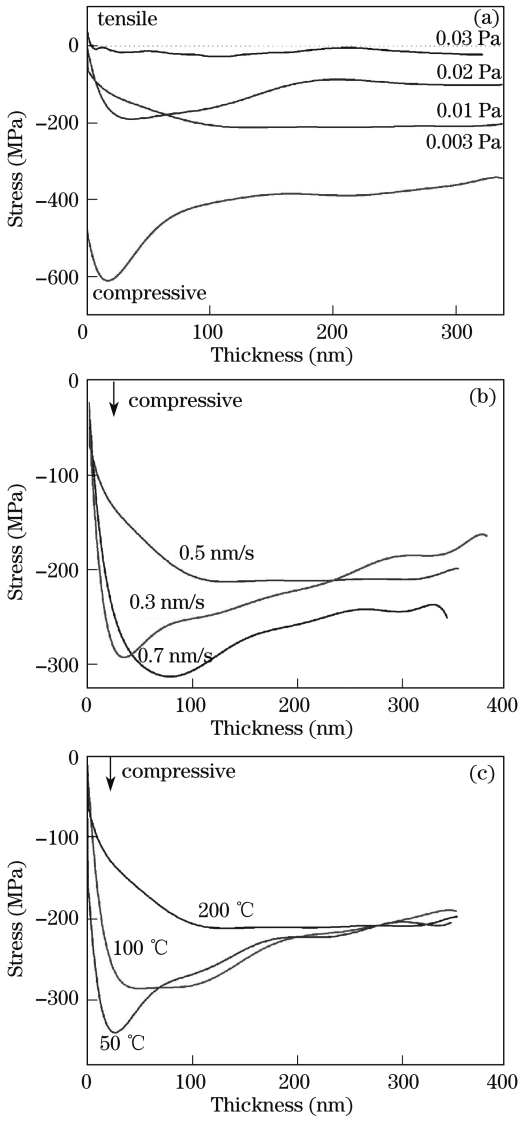

Fig. 1. Evolution of growth stress of films in the deposition process with (a) growth gas pressure from 0.3×10^{-2} to 3×10^{-2} Pa (0.5 nm/s, 200 °C), (b) deposition rate from 0.3 to 0.7 nm/s (1×10^{-2} Pa, 200 °C), and (c) ambient temperature from 50 to 200 °C (1×10^{-2} Pa, 0.5 nm/s).

the ambient temperature.

A typical stress evolution pattern of the SiO_2 monolayer is illustrated in Fig. 2. Based on the physical process and features, the preparation was sequentially divided into five subprocedures: 1) the process of thin film deposition, 2) stopping deposition, 3) lowering the temperature, 4) venting the vacuum chamber, and 5) exposing coated optics to the atmosphere. These subprocedures are marked out by four dotted vertical lines.

A stable state stress of about –340 MPa was obtained with a thickness of more than 100 nm, close to the results of *ex situ* stress measurements after exposure to the atmosphere[22]. After deposition, the stress increased slightly from –349 to –372 MPa. During lowering the temperature, a thermal stress of –44 MPa was observed. In the fast venting course, a dramatic compressive stress of –100 MPa was introduced into the film, which decayed logarithmically as the film was exposed to the atmosphere.

Further research provides more detailed information on the state of SiO_2 films in the subprocedures, as shown in Fig. 3.

After deposition, the change in stress was in the compressive direction and the amplitude of increment stress was from –10 to –35 MPa.

The stress evolution during cooling is shown in Fig. 2(c). Stress versus ambient temperature is plotted in Fig. 4. The measured value of thermal stress is –44 MPa.

We often calculate the thermal stress as

$$\sigma_{\rm th} = \left(\frac{E_{\rm f}}{1-\nu_{\rm f}}\right)\varepsilon = \left(\frac{E_{\rm f}}{1-\nu_{\rm f}}\right)(\alpha_{\rm f}-\alpha_{\rm s})(T_1-T_0), \quad (1)$$

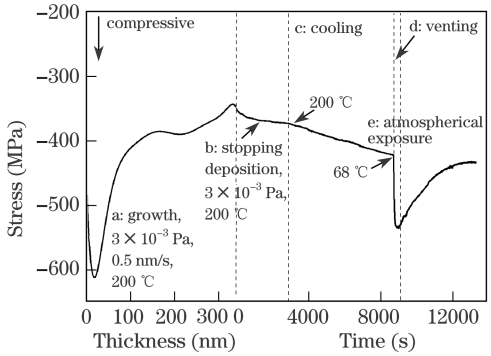

Fig. 2. Schematic representation of the typical evolution of stress of SiO_2 versus thickness or time (a) during deposition, (b) stopping deposition, (c) cooling of sample, (d) venting the chamber, and (e) atmospheric exposure.

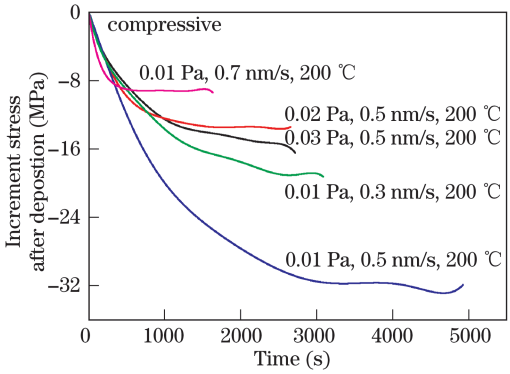

Fig. 3. Stress evolution of SiO_2 film during the stopping deposition subprocedure.

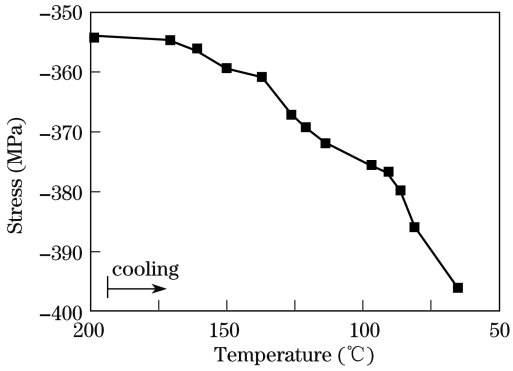

Fig. 4. Stress evolution as a function of ambient temperature in the cooling process.

where $E_{\rm f}$ and $\nu_{\rm f}$ are Young's modulus and Poisson's ratio of thin film, respectively; $\alpha_{\rm s}$ and $\alpha_{\rm f}$ are expansion coefficients of substrate and film, respectively; T_1 and T_2 are the temperatures of the deposition process and stress measurement, respectively. We often assume the deposition condition-independent $E_{\rm f}$, $\nu_{\rm f}$, $\alpha_{\rm s}$, and $\alpha_{\rm f}$ to estimate the thermal stress.

In the cooling subprocedure, we lowered the ambient temperature from 200 to 68 °C. The parameters of substrate and films were taken to be[22]: $E_{\rm f}=73$ GPa, $\nu_{\rm f}=0.162$, $\alpha_{\rm s}=0.7\times10^{-6}$ K^{-1}, $\alpha_{\rm f}=7.2\times10^{-6}$ K^{-1} (20–300 °C); we obtained $\sigma_{\rm th}=-72.5$ MPa.

In the overall venting and exposure process, the reading of QCCO rose continuously from 330.8 to 566.5 nm. Analyzed in combination with the pressure, the compressive stress was found to increase rapidly as the air charging valve was opened (after 2.0 Pa). While a notable change in the reading of QCCO was observed after the pressure reached 310 Pa, a peak of –216 MPa was reached before the end of venting was observed. The stress started to develop into the tensile direction until the end of the experiment. The final stress was compressive and the amplitude was –98 MPa.

The final structures of evaporated films can range from single crystal films and polycrystalline films with columnar or equiaxed grains to largely amorphous films. The fundamental factors governing the microstructure of evaporated films are the kinetic energy of deposited particles and the thermal energy supplied to the deposited film. Film stress is an extremely structure-sensitive property, thus it changes with the deposition method used and the environmental constraints imposed. Even if several attempts have been made to point out general trends in the evolution of stress, most researchers have come to the conclusion that each combination of material or deposition process requires special study.

The features of growth stress shown in our experiments can be interpreted as follows. Firstly, the deposition rate ranging from 0.3 to 0.7 nm/s would not substantially change the kinetic energy of deposit particles. Secondly, the low homologous temperature (ratio of the deposition temperature to the melting point of the evaporated material) from 50 to 200 °C would not substantially change the thermal energy supplied to the deposited film. Thirdly, the residual gas pressure can affect the kinetic energy of condensing particles dramatically. For example, under such conditions as SiO_2 evaporating in 1600 °C, with a source-to-substrate distance of $d=$ 700 mm, the increase of oxygen pressure from 3 to 20 Pa can decrease the incident energy from 200 to 25 meV[8]. Fourthly, a very low but still compressive stress of –20 MPa is observed when the kinetic energy of incident particles is further decreased owing to its low structural integrity.

For the venting and exposure process, the rapid increase in film quality illustrates that the charged air enters the porous film and changes the film structure. However, inversion of the stress developing direction after saturation suggests a complex process. The following two-factor model is applied to analyze the evolution.

Firstly, a continuously increasing compressive component dominates through the adsorption of polar molecules (such as H_2O) in porous SiO_2 film[20]. A model given by

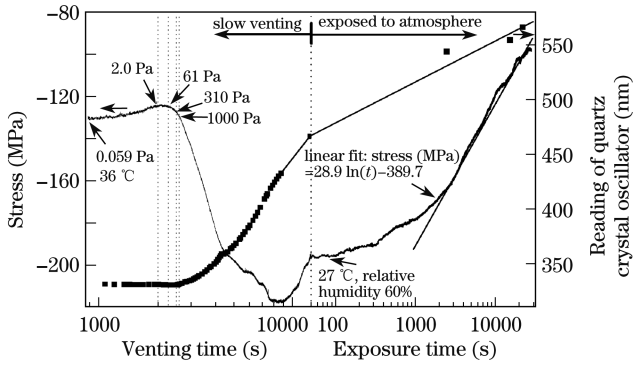

Fig. 5. Stress evolution (fine line, left axis) and reading of the whole thickness of quartz crystal controlled oscillator (solid square line, right axis) versus time (logarithm scale for venting and exposure, respectively).

Hirsch predicts this water absorption-induced stress[17] :

$$\sigma = \frac{6\beta^2 I}{10\pi\varepsilon\alpha^2}, \tag{2}$$

where α is the diameter of pores in porous film, β is the effective dipole moment in the unit area, and I is the integral of interaction force.

Secondly, a gradually increasing tensile component holds the leading state when the water molecule density is high enough to promote the hydration reactions of SiO_2 and H_2O.

A profound analysis of hydration in SiO_2 was provided by Leplan *et al.*[11] In his stress data, the residual stresses of evaporated SiO_2 film vary from –240 to –120 MPa after being exposed to the air from 0.2 to 8 h. In our data, the stress evolution from –196 to –98 MPa after exposure to air from 0 to 8.3 h is shown in Fig. 5. We can also use the model developed by Leplan to linearly fit the stress evolution to the logarithm of time from 0.6 h:

$$\sigma = 28.9\ln(t) - 389.7. \tag{3}$$

With *in situ* stress measurement, we can continuously detect the stresses of the two phases and the saturation phase. This is an effective way that merits further investigation.

For the post-deposition, there is a stress variation during the same time scale for the SiO_2 film observed in polycrystalline Cu film[15]. However, the changing direction is different, and the amplitude of increment stress is far less than that of Cu film. In cooling, the observed stress change is somewhat lower than the theoretically estimated thermal stress. This may be due to a more complex stress behavior. Further studies on these two subprocedures are planned.

In conclusion, the evolution of stresses in evaporated SiO_2 films during the overall preparation has been investigated as a function of different conditions by *in situ* stress measurement. The overall process has been divided into five subprocedures: depositing the atom by vapor, stopping deposition, lowering the temperature of samples, venting the chamber with gas, and exposing the sample to the room air. Compared with deposition rate and temperature, residual gas pressure has more extensive effects on the growth stress. In stopping the deposition process, fast decay is observed in the compressive direction. In the venting and exposure process, the stress is initially increased compressively and then reversed to the tensile direction. This phenomenon is attributed to the combination of the physical and chemical mechanisms of water-induced stress. The compressive component is caused by the admission of polar molecules and the tensile component is caused by the generation of silicic acid.

The authors wish to thank SCHOTT AG for providing the D263T sheets. This work was supported by the National Natural Science Foundation of China under Grant No. 10704078.

References

1. L. B. Freund and S. Suresh, *Thin Film Materials: Stress, Defect Formation and Surface Evolution* (Cambridge University Press, Cambridge, 2003).
2. Y. Chen, W. Zheng, W. Chen, S. He, and Y. Chen, Opt. Optoelectron. Technol. (in Chinese) **3,** (3) 58 (2005).
3. S. Tamulevicius, Vacuum **51,** 127 (1998).
4. J. A. Thornton, Thin Solid Films **54,** 23 (1978).
5. S. Y. Shao, J. D. Shao, H. B. He, and Z. X. Fan, Opt. Lett. **30,** 2119 (2005).
6. Y. Shen, S. Shao, H. He, J. Shao, and Z. Fan, Chin. Opt. Lett. **5,** S272 (2007).
7. Y. Wang, Y. G. Zhang, W. L. Chen, W. D. Shen, X. Liu, and P. F. Gu, Appl. Opt. **47,** (13) C319 (2008).
8. H. Leplan, B. Geenen, J. Y. Robiic, and Y. Pauleau, J. Appl. Phys. **78,** 962 (1995).
9. Q. Xiao, H. He, S. Shao, J. Shao, and Z. Fan, Acta Opt. Sin. (in Chinese) **28,** 1007 (2008).
10. Q. Xiao, S. Shao, J. Shao, and Z. Fan, Chinese J. Lasers (in Chinese) **36,** 1195 (2009).
11. H. Leplan, J. Y. Robic, and Y. Pauleau, J. Appl. Phys. **79,** 6926 (1996).
12. J. A. Floro and E. Chason, Appl. Phys. Lett. **69,** 3830 (1996).
13. C. Friesen and C. V. Thompson, Phys. Rev. Lett. **89,** 126103 (2002).
14. E. Chason, B. W. Sheldon, and L. B. Freund, Phys. Rev. Lett. **88,** 156103 (2002).
15. A. L. Shull and F. Spaepen, J. Appl. Phys. **80,** 6243 (1996).
16. J. Thurn and R. F. Cook, J. Appl. Phys. **91,** 1988 (2002).
17. E. H. Hirsch, J. Phys. D: Appl. Phys. **13,** 2081 (1980).
18. A. E. Ennos, Appl. Opt. **5,** 51 (1966).
19. Y. Shen, Z. Han, J. Shao, S. Shao, and H. He, Chin. Opt. Lett. **6,** 225 (2008).
20. Y. Pauleau, Vacuum **61,** 175 (2001).
21. M. Fang, S. Shao, X. Shen, Z. Fan, and J. Shao, Acta Opt. Sin. (in Chinese) **29,** 1734 (2009).
22. S. Shao, "Study of the origin mechanism and controlling method of stress in thin films" PhD Thesis (Shanghai Institute of Optics and Fine Mechanics, Shanghai, 2005).